Geophysical Journal International

*Geophys. J. Int.* (2023) **235,** 942–950
Advance Access publication 2023 July 12
GJI Applied and Marine Geophysics

https://doi.org/10.1093/gji/ggad286

# Exploiting image logs to reduce drilling hazards: an innovative Artificial Intelligence methodology applied in East Africa

Attilio Molossi and Michele Pipan

*Dipartimento di Matematica e Geoscienze, Università di Trieste, Via E. Weiss* 1, *Trieste* 34128, *Italy. E-mail: attilio.molossi@phd.units.it*

Accepted 2023 July 6. Received 2023 June 30; in original form 2022 September 30

## SUMMARY

Image logs are crucial for petrophysical and structural characterization of drilled formations. Logging while drilling (LWD) image logs allow near real-time characterization of formations during drilling. Interpretation time required by humans can become critical, as structural interpretation provides the most crucial information for decision-making steps with respect to drilling operations. An example of this occurred in a deepwater system of reservoirs in East Africa. During the drilling of some wells, drilling was interrupted by unexpected borehole stability issues observed in a mass transport deposit. Those problems can detrimentally affect operations by impacting the efficiency of drilling. Therefore, a procedure for the automation of LWD data analysis was developed aimed at reducing drilling risk associated with borehole stability. A workflow is proposed based on an innovative assortment of AI methodologies for automatic real-time interpretation of LWD image log, applied to density image logs. The goal is to mimic manual human dip picking, combining computer vision, numerical series analysis and machine learning. Computer vision techniques are applied to detect the main density contrasts, representing the most likely surfaces. Sharp contrasts in the image are then investigated by dynamic time warping for similarity analysis. Finally, the geological plane is defined as a regression plane passing through the most similar contrasts, and a surface confidence criterion is defined based on the homogeneity of contrast along the curve suggested by the regression. Feature identification by a geologist was used as benchmark for comparison and metrics. Accuracy is referred to the difference between apparent dip and azimuth of geological surfaces coming from human and automated workflows, following the idea that two similar geometric results would eventually lead to equally similar geological considerations, and thus to similar operational measures. In general, a prediction accuracy of 60 per cent for the tested wells is observed, considering the total set of surfaces coming from the model. Nevertheless, the results suggest a positive correlation between the apparent dip of the discontinuities and the model error and a general less confidence for the surfaces with greater dip. By isolating the subset of low dipping features generated by the model, that is up to 35°, the accuracy appears to increase up to more than 70 per cent, suggesting that correlation is more difficult for high dipping geological planes. This class of curves also shows a general lower confidence and much of this latter class of surfaces are more likely to be found in the depth interval in which borehole stability issues occurred.

**Key words:** Composition and structure of the continental crust; Composition and structure of the planets; Fracture and flow; Microstructure; Machine learning; Downhole methods.

## 1 INTRODUCTION

Images of the borehole are obtained by logging and data processing methods, resulting in a centimetre-scale image of the borehole wall (Sun *et al.* 2021). The wireline tools, which can produce resistivity images, ultrasonic images or a combination of the two, are lowered into the well and the measurements are made either while running in the hole (ultrasonic images only) or up-hole (resistivity, combined ultrasonic and resistivity images). Logging while drilling (LWD) tools are part of the rotating borehole assembly and can generate resistivity, ultrasonic, density and gamma ray images. LWD and wireline data differ in terms of image quality and resolution.

Higher resolution wireline images can be interpreted at the centimetre-scale whereas lower resolution LWD images (Fig. 2)

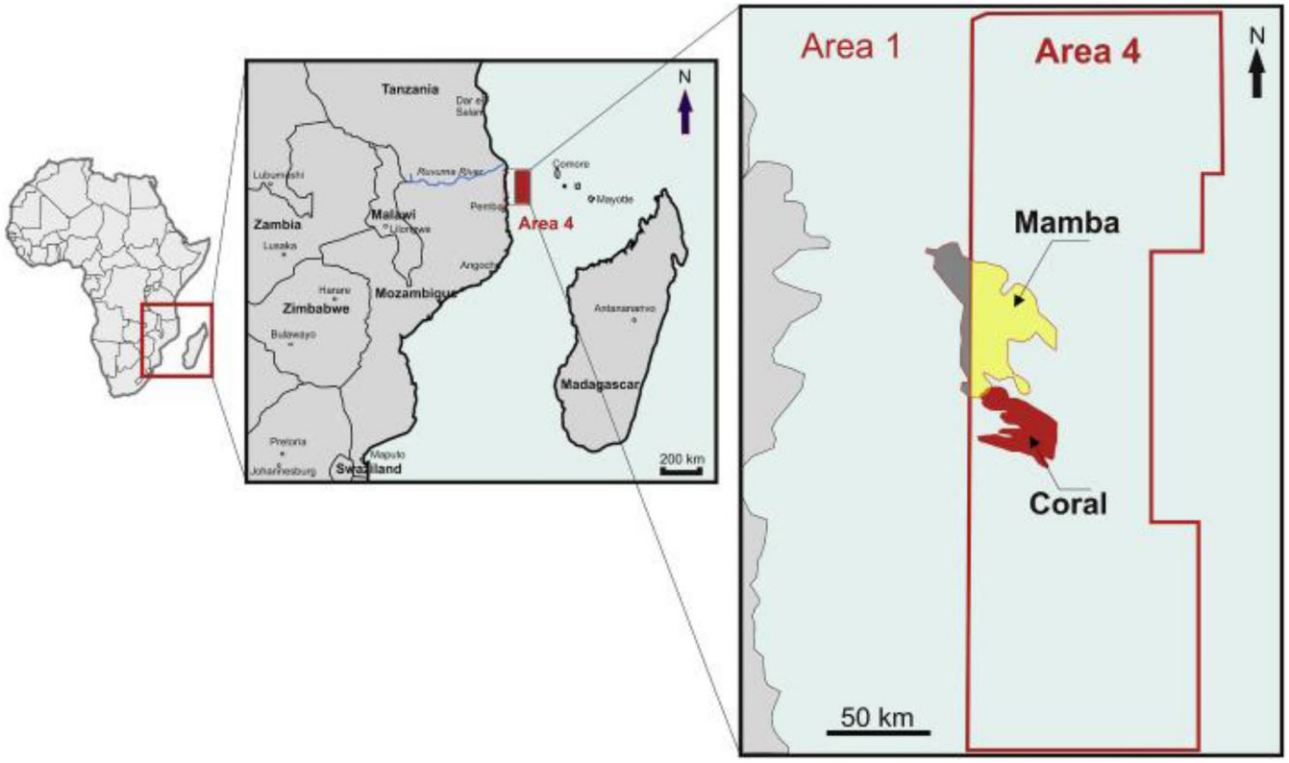


**Figure 1.** The gas fields in Northern Mozambique were found in deepwater clean sands reservoirs, comprising turbiditic deposits interacting with bottom currents. Area 4 was discovered by Eni in 2011 and 2012 (from Fonnesu *et al.* 2020).

can only be resolved at the decimetre to metre-scale. Density image logs like those that were used in the development of this method are produced by azimuthal LWD tools. In our case, the tool technology divides the 360° of the borehole into 16 sectors, one for each 22.5°. The tool measures the formation bulk density in each sector by introducing gamma rays into the formation with a radioactive source and counting the rate of gamma rays scattered back to a near and a far detector (Shahinpour 2013). This data is used to derive structural and lithological information in real-time, during the drilling of a borehole. Modern LWD imaging tools are now mature enough to be used for a variety of applications, including real-time reservoir characterization and field optimization. Such applications indicate the importance of this type of data for a variety of purposes. Information from image logs can be integrated, for example, into crucial decision-making phases such as geosteering (Mathis *et al.* 2003; Poppelreiter *et al.* 2010; Mukherjee 2018). Before being processed for interpretation purposes, LWD image logs must pass through a quality check. LWD instruments acquire data at regular time intervals during drilling and are equipped with an internal clock. However, the drilling speed is subject to variations related, for example, to variable resistance of formations, so LWD images can be affected by artefacts (such as flattening or stretching of features in the image). At the surface a depth tracking system, also equipped with a clock, monitors the time and depth of drilling, based on the length of the drill string and the position of the top drive in the derrick. The synchronization of the downhole and uphole clocks allows the corrections of the artefacts, by merging the time-depth data from the surface system with time-measurement data from the tool, to get the best depth-measurement data. The next processing step is to set a maximum and minimum value for the petrophysical parameter measured by the tool, to represent the data in a colour scale (e.g. light is high value and dark is low value as in Fig. 2). The colour scale used to represent the data is defined between these two extremes. The colour scale is normalized over the entire acquisition interval to produce statically normalized images and then again over arbitrarily sized windows, to produce dynamically normalized images. The statically normalized shows the overall variations of properties measured by the LWD tool, whereas the dynamic normalization highlights the details.

The interpretation of such image data aims to identify geological features such as layers, fractures and faults as planar features intersecting the borehole, that will appear as sinusoids on an unwrapped image.

Apparent dip azimuth and dip magnitude of all picked features can be determined using eq. (1) (Luthi 2001; Mukherjee 2018)

$$Dip = \text{arctg}\frac{H}{D}, \tag{1}$$

where $H$ is the height of the sinusoid (amplitude) and $D$ the diameter of the borehole. Due to well deviation, those are apparent parameters and need a conversion to real values (Bergt 1995). For the purposes of this work LWD azimuthal density image logs were interpreted manually and by an automated interpretation system that will be described later in Section 2. LWD azimuthal density images were chosen for the implementation of an automatic system because their interpretation allows direct detection of geological discontinuities during drilling, which can support drilling risk reduction helping in the early detection of dangerous conditions that can undermine borehole stability.

The automated interpretation system discussed in this work has been considered as a solution for real-time image log processing and a support to human interpreters for fast structural and geological

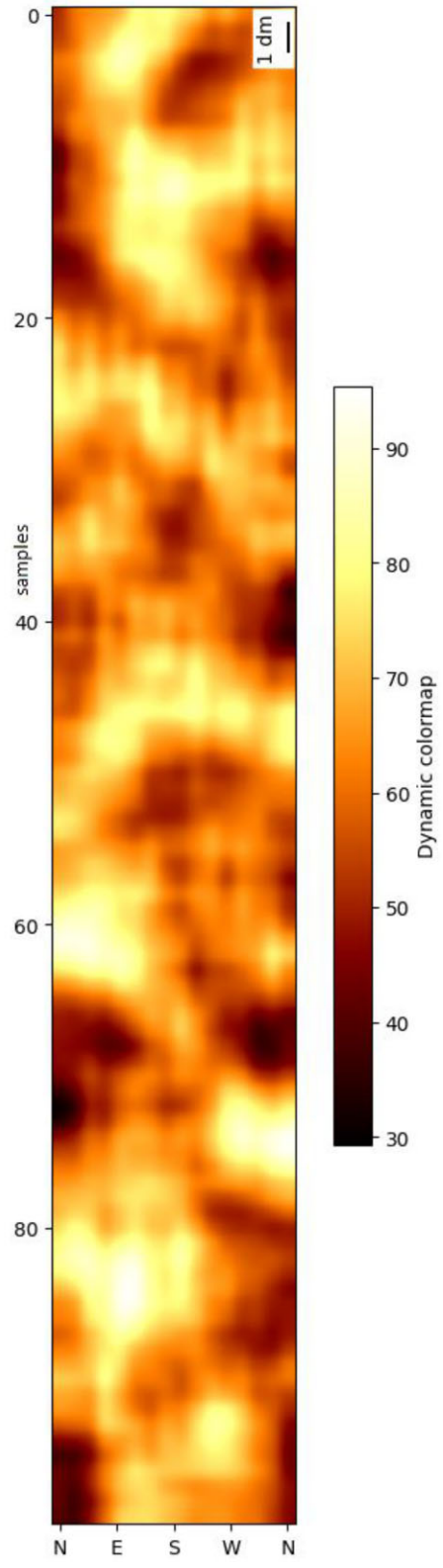


**Figure 2.** Example of a LWD density image log comprising a 5 m interval displaying geological features that will be manually interpreted. Note low feature resolution. The dark colour corresponds to low density and vice versa.

characterization, thus providing helpful insights for field optimization purposes. Specifically, this work was inspired by borehole stability problems that occurred in a mass transport complex (MTC), henceforth referred to as MTC370, during the drilling of an offshore well in East Africa (Fig. 1). The borehole instability occurred within an interval of sand channel complexes containing convolute, chaotic and weak seismic reflections (Fonnesu *et al.* 2020). According to the depth where the borehole stability issues occurred, they resulted associated with the MTC370. The objective of the method is therefore to provide a real-time image log analysis system, that can aid the interpreter with early detection of these types of deposits that are risky for drilling due to their general heterogeneity and intense fracturing. The methodology is an integration of edge detection and similarity analysis. It was tested on two wells, hereinafter referred to as well 7 and 8, that are approximately 2 km apart, where the MTC370 limits were manually pre-interpreted on the associated LWD density image logs.

Edge detection encompasses numerous useful methods for simplified image analysis, for the recognition of contours or edge points in an image, aimed at many applications (Canny 1986), including the use of the results of an edge detector as input for pixel or edge matching for object recognition in digital images (Marr 1978).

In Itakura (1975) the effectiveness of a minimum cumulative distance measure between two patterns for speech recognition purposes is demonstrated. In Sakoe & Chiba (1978) the success of dynamic programming (DP) in the pattern-matching algorithm for speech recognition purposes is also demonstrated. Dynamic time warping (DTW) is a method to obtain alignment of two time series, following DP principles, by means of non-linear deformation of the two sequences (Muller 2007). The discussed system is based on the combined application of edge detection and DTW. Details of this procedure are explained in Section 2.

## 2 DATA AND METHODS

The dataset on which our workflow was developed consists of LWD image logs coming from well 7 and well 8 (see Section 1). For each borehole a manual interpretation was first performed focusing on the most obvious features, that is the sharpest density contrasts.

The results of the manual approach were used as a baseline for comparison with the model results in terms of apparent dip magnitude and dip azimuth. The apparent parameters were considered because they can be derived directly from amplitude and phase of the sinusoids that represent the planar approximation of the identified geologic features. To derive the true values, well position and inclination must be determined from measurements while drilling (MWD) data, which generally include magnetometer and inclinometer data acquired during drilling.

Manual interpretation was done using Geolog (E&P). This software allows the interpreter to pick the points on the interpreted surface and automatically performs the fitting of sinusoids. It also computes both the apparent and the true dip magnitude and dip azimuth of the interpreted surface and allows for its geological classification (e.g. bedding, fracture and fault). The automated system processes the image logs and correlates the geological features detected around the wellbore but does not classify them according to their geological significance. The automated correlation of sinusoids is based on an idea of similarity between pairs of numerical series among the 16 sectors covering the 360° of the borehole. This method is a combination of edge detection and DTW for the determination of similarity between portions of numerical series. The

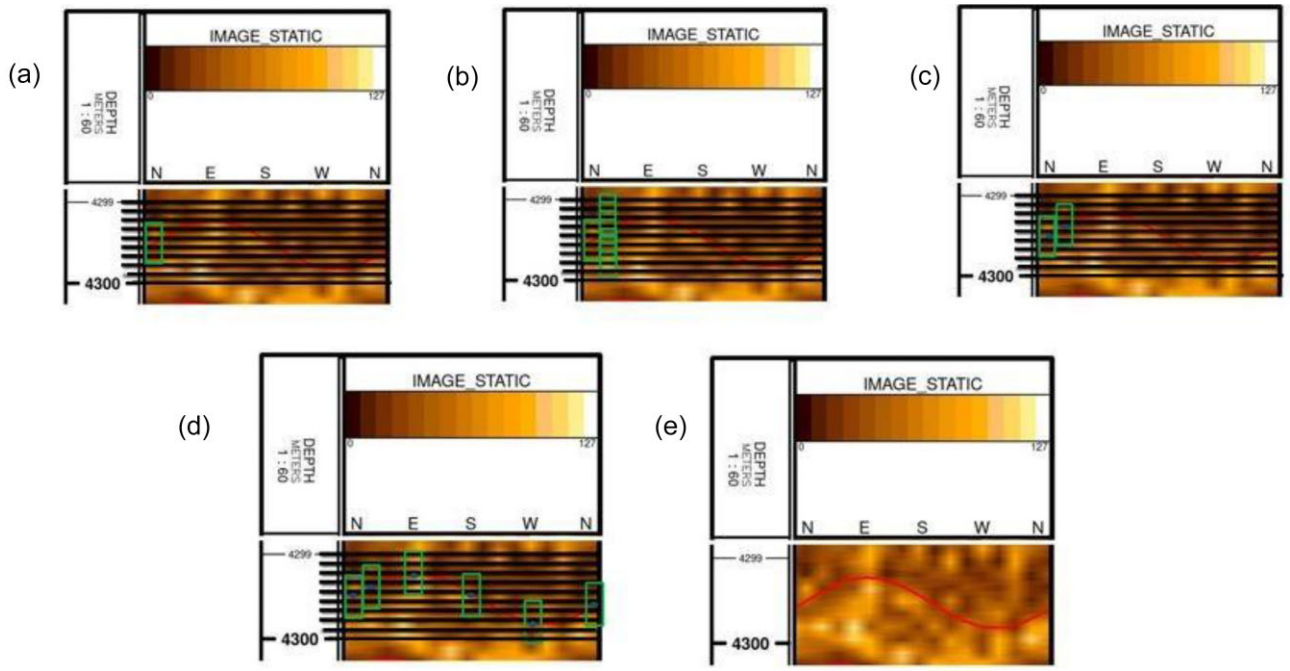


**Figure 3.** Summary of the main steps used by the algorithm to identify planar geological features in the LWD image log. (a) Centre a 50 cm window in a point of interest, (b) calculate the similarity with sliding windows in the next sector and, (c) keep the coordinates of the window with maximum similarity, (d) repeat for all the sectors in the image to get the scatter of similar points and (e) correlate the planar feature by fitting a sinusoidal curve.

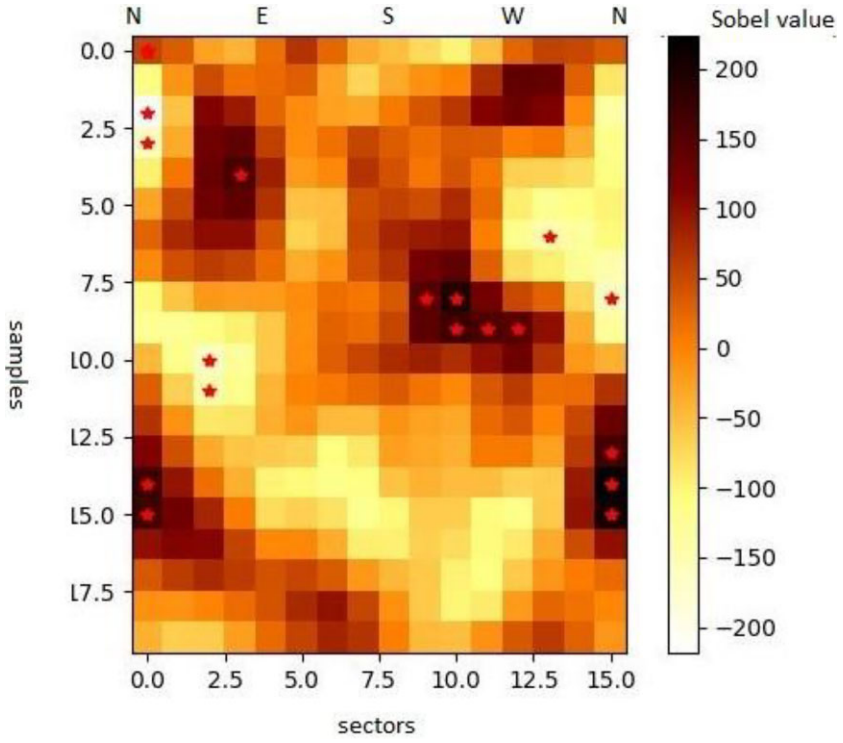


**Figure 4.** Example of application of a Sobel operator to the LWD data of Fig. 2: red points represent the point of interest set, to start the feature correlation.

automated flow, described in Fig. 3, starts from edge detection with the Sobel operator. This is an efficient differential gradient edge detector that estimates local intensity gradients in the image with the help of appropriate convolution masks. To obtain the sinusoids at density contrasts, the edges found by the Sobel operator are used as input for the calculation of similarity between portions of the image and automatic surface detection. In this way we extrapolated from the image what we called the points of interest (see Fig. 4).

These points of interest identified by the Sobel operator are used as starting points for the calculation of similarity using the DTW technique (as described in Fig. 3). This technique warps two generic sequences to reach their match by finding the optimal warping

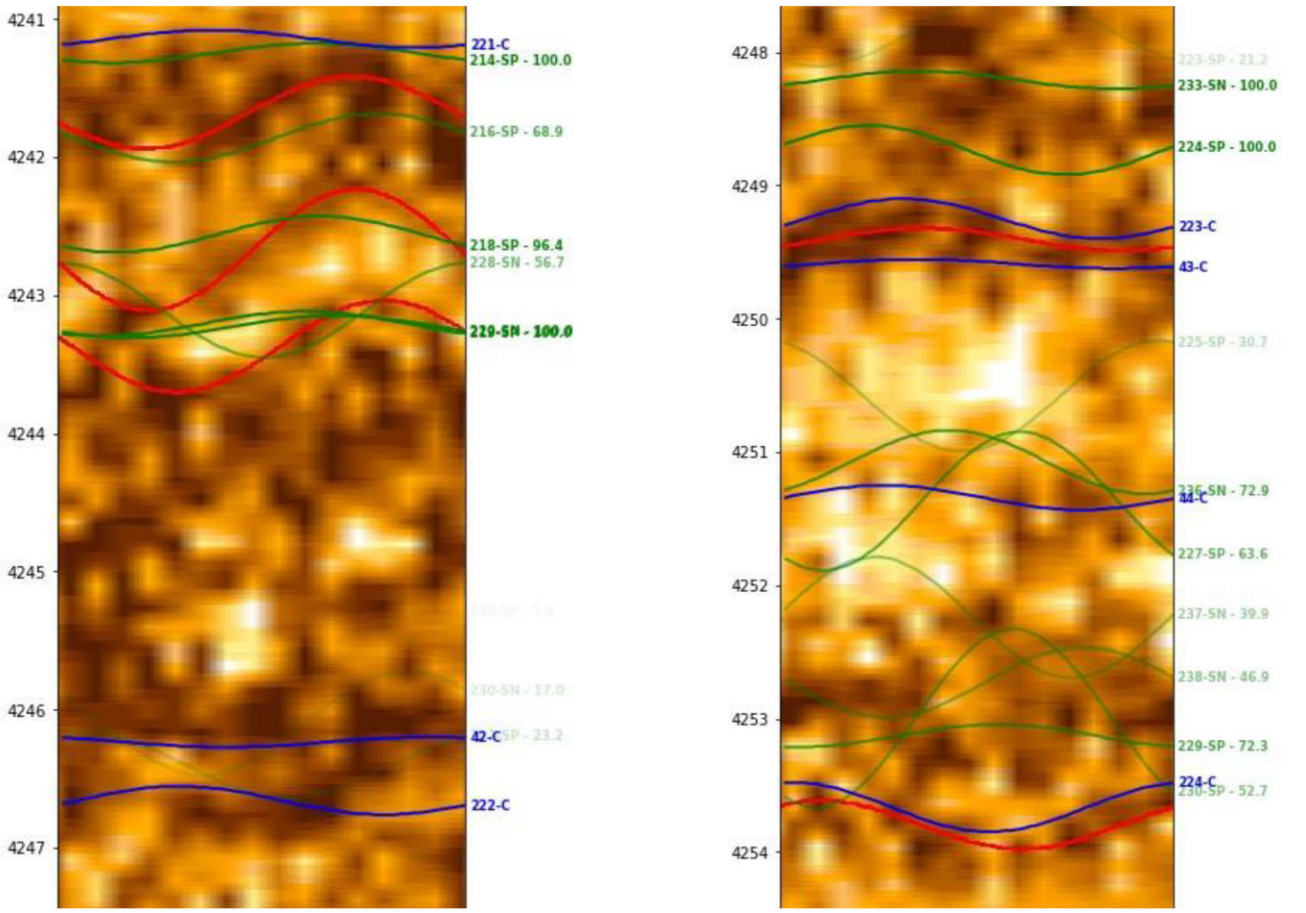


**Figure 5.** Example interval from MTC370, well 8. The algorithm results are plotted, together with specific ID and confidence values for each surface. Transparency of the curves is proportional to confidence, with the more transparent indicating lower confidence. Blue curves result from edge detection, green curves come from regressions and red curves come from basic human interpretation.

function of the independent axis, which also corresponds to the minimum cumulative distance between the sequences. The similarity is repeatedly calculated between a so-called target sequence, centred at one point of interest, and a set of input sequences in the next sector. The general procedure is as follows: first, a target sequence block is centred at one point of interest (this will be repeated for each point of interest). The target block has the point of interest in the centre and includes 5 samples (25 cm) above and below the centre in the same sector. Ten samples in the target sequence correspond therefore to 50 cm on the corresponding density series, centred in a point of interest. The algorithm then defines an input sequence block on the adjacent sector, having the same extension and slides it sample-wise from 1 to 5 samples above and below the depth of the target sequence block. For each of these input blocks, the similarity with the target block is calculated. The aim is to identify in the adjacent sectors the portion that has the maximum similarity with the target block within a 1-m window. The most similar input block is determined by means of the similarity measure based on DTW and, specifically, it corresponds to the input block showing the minimum DTW distance with respect to the target block. Once identified, the input sequence block with maximum similarity is used as the new target block, and the procedure is repeated with respect to the next sector, iteratively, until all 16 sectors are covered.

At the end of all the iterations, we have a set of centroids corresponding to the most similar blocks for each point of interest. A least square regression method is applied after coordinate transformations from 2-D to 3-D to find the best-fitting sinusoid, that is the best approximation of a planar feature. Finally, the distribution of the Sobel values along the correlated surfaces was used as a criterion to assess the confidence. Ideally, in fact, the Sobel value is assumed constant for each density contrast in the image. In practice, this may not be true especially because of the low LWD image log resolution. Therefore, the confidence for each surface was calculated as the percentage of points along the surface with the same sign of the Sobel value. The confidence of the surfaces ranges from 0 to 100 and is generated by the algorithm together with the ID of the curves and their apparent dip magnitude and dip azimuth (see Fig. 5). Those quantities were used as parameters for the model evaluation. The mismatch between the apparent dip azimuth and dip magnitude of manual and model surfaces was used to define an error for the orientation of features generated by the model. Manual interpretation showed different grades of heterogeneity in the drilled interval and we can clearly distinguish the reservoir, comprising homogeneous and clean sandy layers with a thick, heterogeneous and chaotic unit at the top. This heterogeneous unit was interpreted as the mass transport deposit described at the end of Section 1, referred to as MTC370. In this deposit, manual interpretation showed a higher mean dip magnitude and greater dip azimuth dispersion of the correlated geologic features. To support early detection of heterogeneous and chaotic formations, that are risky for drilling operations, the algorithm also includes a function

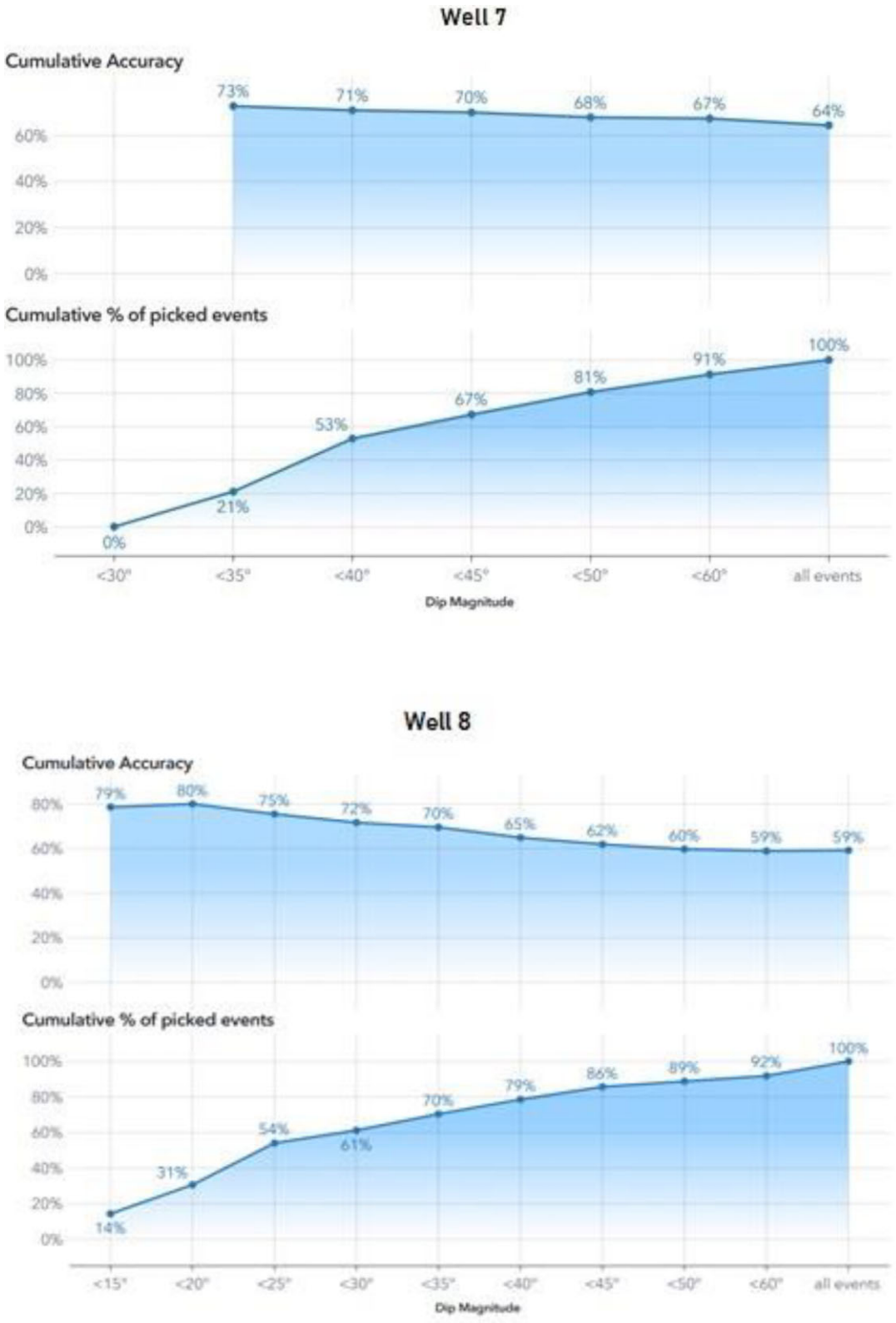


**Figure 6.** Accuracy as a function of dip magnitude of the retrieved surfaces shows a positive correlation between model error and dip, for both wells. Metrics show general robustness from well to well.

that calculates the percentage of features with dip magnitude greater than 45° and the percentage of features with confidence less than 75 per cent. The algorithm checks if the percentages of features meeting the conditions are greater than 50 per cent in 10-m windows and an alerting system highlights which of these conditions is verified in each window as in Fig. 7.

The density contour stereonets of the apparent dip magnitude and dip azimuth resulting from manual interpretation

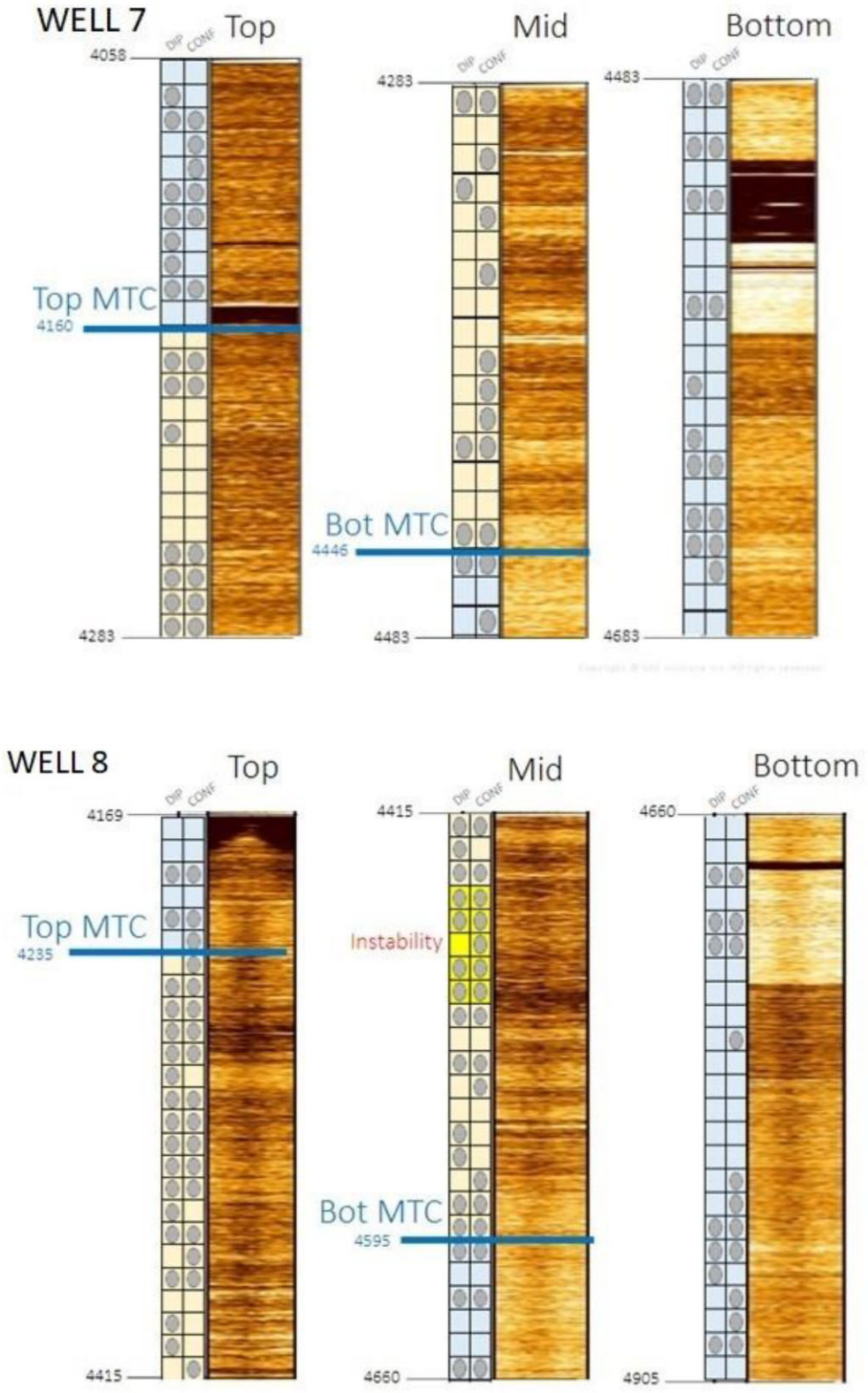


**Figure 7.** Mass transport deposit detection system shows good performance in detecting the MTDs and in particular the interval that gave unforeseen borehole stability issues.

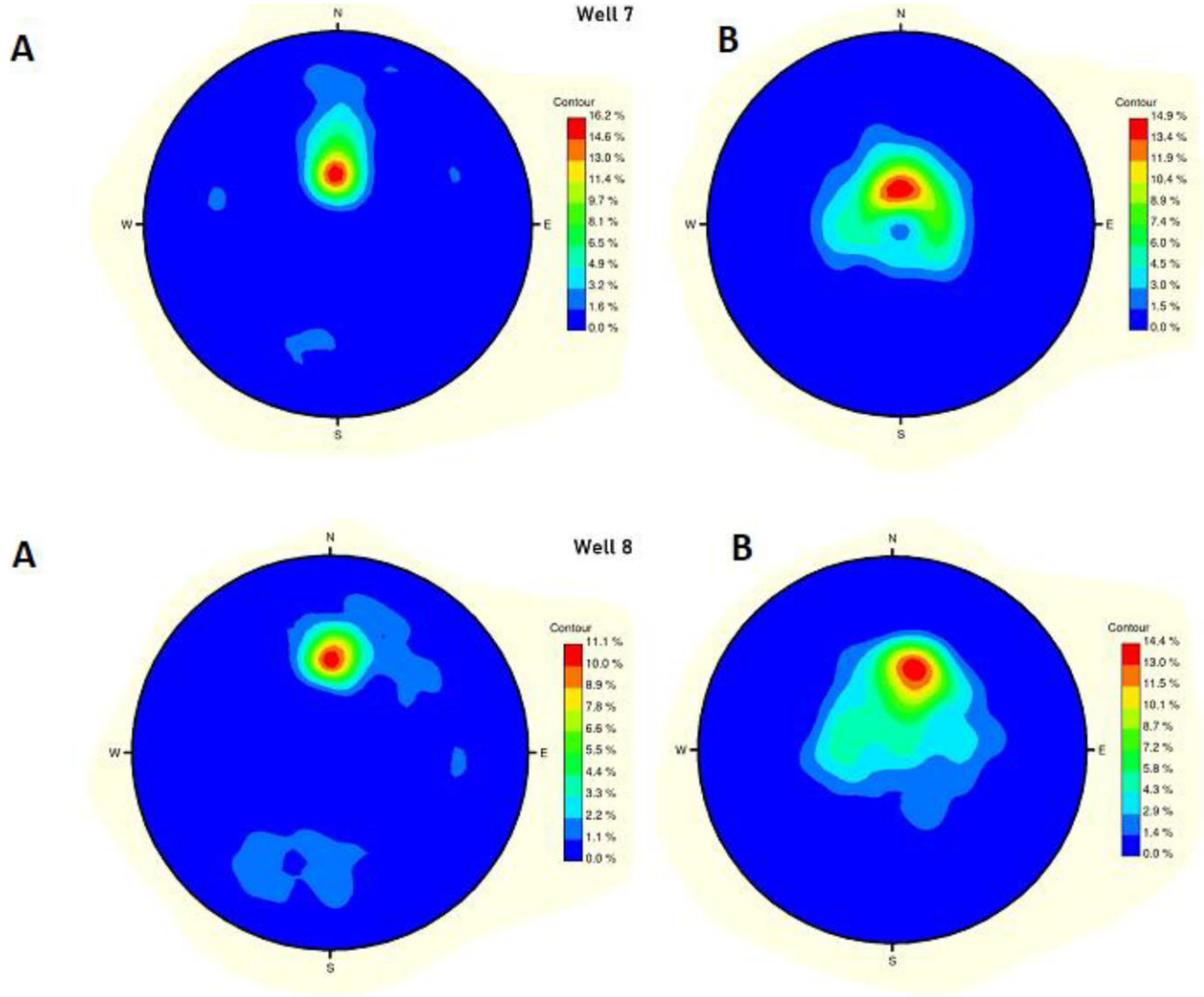


**Figure 8.** Stereonet plot (upper hemisphere) showing the dip angles and dip azimuths of the features picked on the borehole LWD density image. (a) Manually picked dip data set showing a dominant dip azimuth towards north. (b) Model processed dip more dispersed azimuths that broadly agree with manually picked dips.

were compared with those resulting from the model for the evaluation.

## 3 RESULTS

The performance of the model was assessed with the calculation of metrics, based on the comparison between the basic manual and model results. The model identified a greater number of features in the image than the basic manual interpretation (see Fig. 5). Values of apparent dip magnitude and dip azimuth of the sinusoids were used to define errors. We tested the algorithm on the two wells and observed an average prediction accuracy of 61 per cent for dip magnitude and an average error of predicted azimuth of 40°, for the whole set of identified geological features (Fig. 6). Accuracy assessed for features with an apparent dip magnitude lower than 35°, which represent the 70 per cent of the total number of curves, went from 61 to 70 per cent. For the apparent dip azimuth parameter, the average error decreased from 40° to 19° (Fig. 6). Note that this means that the error is less than one sector (22.5°).

Fig. 7 shows that in the interval where borehole instability occurred the algorithm detects the MTC in four out of a total of five 10-m-long windows, showing that the MTC identification criteria based on the apparent dip magnitude and the confidence of the geological features can be efficient (see Section 2). Stereonets from manually picked and automated analysis (with 100 per cent confidence) showed a general higher dispersion observed in the AI data (Fig. 8). This may be due to the greater number of features identified by the AI method, however the two dip picking techniques display a general agreement.

This result illustrates the potential of this system to predict a realistic structural and geometrical scenario from noisy and low-quality LWD image log, hence highlighting its applicability to risk reduction during drilling.

## 4 CONCLUSIONS

In conclusion, an innovative methodology was implemented on LWD density image logs for real-time automated data-analysis aimed at reducing risks of borehole instability. The methodology

was developed to simulate the interpretation process using a combination of computer vision and similarity analysis.

The combination of edge detection (Sobel operator) and DTW methods was able to emulate the process of geological feature identification in LWD images. At the current stage of development, the system can detect more surfaces than a basic manual interpretation. In addition, the system includes an efficient function to report disorder and heterogeneity of drilled intervals, based on confidence and average dip magnitude of surfaces within 10-m windows. As a result, the system correctly reports intervals where borehole stability problems had occurred and therefore, we can say that it would have helped the interpreter to promptly recognize risky units for operations.

However, further improvement is still required to increase model accuracy in predicting apparent dip of surfaces, which is crucial to support real-time discrimination of bedding and fracture/fault surfaces. Fault and fracture classification is important for risk for drilling operations and borehole stability. Furthermore, this algorithm has so far been tested only on azimuthal density LWD image logs but should also be tested on other types of LWD images (such as GR or resistivity) on which we expect it to be applicable.

## ACKNOWLEDGMENTS

I would particularly like to thank Davide Baldini, Eni, for his supervision and corrections, Federica Citterio and her colleagues of SAS, for her technical support on data management and automation design.

## DATA AVAILABILITY

Original data were collected by Eni and cannot be shared due to confidentiality agreement.

## REFERENCES

Bergt, D. 1995. Resistivity measurements at the bit provide real-time formation evaluation before invasion. *J. Petrol. Techol.,* **47**(6), 492–492.

Canny, J. 1986. A computational approach to edge detection, *IEEE Trans. Pattern Anal. Mach. Intell.,* **PAMI-8**(6), 679–698.

Fonnesu, M., Palermo, D., Galbiati, M., Marchesini, M., Bonamini, E. & Bendias, D. 2020. A new world-class deep-water play-type, deposited by the syndepositional interaction of turbidity flows and bottom currents: the giant Eocene Coral Field in northern Mozambique. *Mar. Petrol. Geol.,* **111,** 179–201.

Itakura, F. 1975. Minimum prediction residual principle applied to speech recognition, *IEEE Trans. Acoust., Speech, Sig. Process.,* **23**(1), 67–72.

Luthi, S. M. 2001. Density borehole imaging, geological, in *Geological Well Logs: Their Use in Reservoir Modeling,* pp. 147–153, Springer, Berlin, Heidelberg.

Marr, D.,1978. A computational theory of human stereo vision. *Proc. R. Soc. Lond., B,* **204,** 301–328.

Mathis, B., Leduc, J. P. & Totalfinaelf, T. V. 2003. *Proceedings of the AAPG Annual Convention Salt Lake,* Salt Lake City, Utah, 11–14 May 2003.

Mukherjee, S. 2018. *Teaching Methodologies in Structural Geology and Tectonics,* Springer, pp. 237–251.

Muller, M. 2007. Dynamic time warping, *Inform. Retrieval Music Motion,* **2,** 69–84.

Poppelreiter, M., Garcìa-Carballido, C. & Kraaijveld, M. 2010. Borehole image log technology: application across the exploration and production life cycle, in *Dipmeter and Borehole Image Log Technology,* pp. 1–13, American Association of Petroleum Geologists.

Sakoe, H. & Chiba, S. 1978. Dynamic programming algorithm optimization for spoken word recognition, *IEEE Trans. Acoust., Speech, Signal Process.,* **26**(1), 43–49.

Shahinpour, A. 2013. Borehole image log analysis for sedimentary environment and clay volume interpretation. *Institutt for petroleumsteknologi og anvendt geofysikk*. https://ntnuopen.ntnu.no/ntnu-xmlui/handle/11250/240255

Sun, Q., Li, N., Duan, Y., Li, H. & Tang, H. 2021. Logging-while-drilling formation dip interpretation based on long short-term memory, *Petrol. Explor. Dev.,* **48**(4), 978–986.